

Inequivalence of time and ensemble averages in ergodic systems: exponential versus power-law relaxation in confinement

Jae-Hyung Jeon^{1,*} and Ralf Metzler^{2,1,†}

¹*Department of Physics, Tampere University of Technology, FI-33101 Tampere, Finland*

²*Institute for Physics & Astronomy, University of Potsdam, D-14476 Potsdam-Golm, Germany*

Single particle tracking has become a standard tool to investigate diffusive properties, especially in small systems such as biological cells. Usually the resulting time series are analyzed in terms of time averages over individual trajectories. Here we study confined normal as well as anomalous diffusion modeled by fractional Brownian motion and the fractional Langevin equation, and show that even for such ergodic systems time-averaged quantities behave differently from their ensemble averaged counterparts, irrespective of how long the measurement time becomes. Knowledge of the exact behavior of time averages is therefore fundamental for the proper physical interpretation of measured time series, in particular, for extraction of the relaxation time scale from data.

PACS numbers: 05.40.-a, 02.50.-r, 05.70.Ln, 87.15.Vv

I. INTRODUCTION

Due to recent advances in single particle tracking techniques, analyses based on single trajectory averages have been widely employed to study diffusion in complex systems, e.g., of large biomolecules and tracers in living cells [1]. Examples include the motion in the cellular cytoplasm of messenger RNA molecules [2], chromosomal loci [3], lipid granules [4], and viruses [5], telomeres in cell nuclei [6], or of protein channels in the cell membrane [7]. Under the assumption of ergodicity, i.e., the equivalence of (long) time averages (TA) with ensemble averages (EA), the physical interpretation is often based on the time series analysis of single trajectories. For instance, particle-to-particle diffusion properties are typically studied via TA mean squared displacements (MSD) of individual time series $x(t)$,

$$\overline{\delta^2(\Delta)} = \frac{1}{T-\Delta} \int_0^{T-\Delta} [x(t+\Delta) - x(t)]^2 dt, \quad (1)$$

where Δ is the lag time and T the length of the time series. Invoking ergodicity arguments, it is tacitly assumed that $\overline{\delta^2(\Delta)}$ corresponds to the EA MSD $\langle x^2(t) \rangle$ with the identification $t \leftrightarrow \Delta$, in the limit of long measurement times (i.e., $T \rightarrow \infty$). For *free* normal diffusion one can indeed show analytically that $\langle x^2(t) \rangle = \overline{\delta^2(t)} = 2K_1 t$ as $T \rightarrow \infty$ [11, 12]. At finite T , the result for $\overline{\delta^2(\Delta)}$ will generally show trajectory-to-trajectory variations. However, a similar equivalence still holds when $\overline{\delta^2}$ is averaged over many individual trajectories: $\langle x^2(t) \rangle = \overline{\langle \delta^2(t) \rangle}$ [11]. In what follows we use the symbol $\overline{\delta^2}$ when $T \rightarrow \infty$, and $\langle \delta^2 \rangle$ for finite T , unless specified otherwise. For anomalous diffusion of the form $\langle x^2(t) \rangle = 2K_\alpha t^\alpha$ with anomalous diffusion constant K_α of physical dimension $\text{cm}^2/\text{sec}^\alpha$

and anomalous diffusion exponent α ($0 < \alpha < 2$) [13], the same conclusion holds if the process is described by fractional Brownian motion (FBM) or the fractional Langevin equation (FLE) [14–16].

In contrast, disagreements between TA and EA are not surprising for non-ergodic processes. A prominent example is anomalous diffusion described by continuous time random walks (CTRW) with diverging characteristic waiting times [17–19]: while the EA MSD scales as $\langle x^2(t) \rangle \simeq t^\kappa$ with $0 < \kappa < 1$, the TA MSD grows *linearly* with the lag time, $\overline{\delta^2(\Delta)} \simeq \Delta$ for free motion [11, 12]. Under confinement one observes $\overline{\delta^2(\Delta)} \simeq \Delta^{1-\kappa}$ instead of the saturation plateau of the EA [15, 20, 21]. Recently it was found that the TA MSD of tracers in living cells indeed exhibit such CTRW behavior [4, 7].

Here, we show that *even for ergodic processes* the TA may differ from the EA. This a priori unexpected discrepancy arises from the fact that generally dynamic variables are not well-defined in the TA sense, and therefore care is necessary when interpreting TA based on knowledge about the corresponding EA. We explicitly study this effect for stochastic processes of regular Brownian, FBM, and FLE types, confined in an harmonic potential. Processes of the FBM and FLE kind are closely associated with the motion of tracer molecules in viscous environments, single file diffusion, monomer motion in polymers, or the relative motion of aminoacids in proteins [8]. They have also been identified as stochastic mechanisms for the tracer motion in living cells and reconstituted crowding systems [3, 4, 9, 10].

Consider first an overdamped Brownian particle in the harmonic potential $U(x) = kx^2/2$ of stiffness k . With initial position $x(0) = 0$ the EA MSD is

$$\langle x^2(t) \rangle = (1 - e^{-2kt/\gamma})/[bk], \quad (2)$$

while the EA taken over the TA MSD (1) becomes

$$\begin{aligned} \langle \overline{\delta^2(\Delta, T)} \rangle &= \frac{2}{\beta k} \left(1 - e^{-k\Delta/\gamma}\right) \\ &+ \frac{\gamma}{2k(T-\Delta)} \left(e^{k\Delta/\gamma} - 1\right)^2 \left(e^{-2kT/\gamma} - e^{-2k\Delta/\gamma}\right) \end{aligned} \quad (3)$$

*Electronic address: jeonjh@gmail.com

†Electronic address: rmetzler@uni-potsdam.de

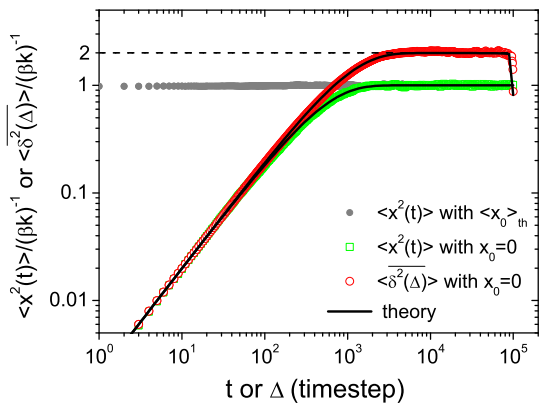


FIG. 1: EA and TA MSD for a Brownian particle in an harmonic potential. Solid lines: Eqs. (2), (3). Symbols: simulations with $\gamma = 1$, $\beta = 1$, $k = 1$, time step $\delta t = 0.001$, and measurement time $T = 10^5$. The flat curve corresponds to thermal initial conditions.

Here γ is the friction coefficient and β the Boltzmann factor. Both quantities are identical initially, before confinement effects come into play: $\langle x^2(t) \rangle \sim 2K_1 t \sim \langle \delta^2(t) \rangle$ with $K_1 = 1/[\beta\gamma]$. However, for $T, \Delta \rightarrow \infty$ (with $T - \Delta \rightarrow \infty$) the TA MSD converges to $\langle \delta^2(\Delta) \rangle \rightarrow 2/[\beta k]$, twice the thermal value $\langle x^2 \rangle_{th} = 1/[\beta k]$. The difference between TA and EA is shown in Fig. 1 for both the analytical results and simulations, with excellent agreement. Note the sudden dip of the TA MSD at $\Delta \approx T$ at the finite measurement time T , at which the limiting behavior $\langle \delta^2(\Delta \rightarrow T) \rangle = \langle x^2(T) \rangle$ is observed. These features are generic for the definition of the TA MSD (1) under confinement, compare Ref. [15, 20].

What results will be obtained for more complicated, non-Brownian motion? We analyze the case of anomalous diffusion governed by FBM and FLE and show that the entire relaxation dynamics is significantly different for the TA, despite the ergodic nature of these processes. Knowledge of the exact behavior of TA quantities is imperative for the correct physical interpretation of time series, in particular, to extract the relaxation time.

II. FRACTIONAL BROWNIAN MOTION

FBM $x_\alpha(t)$ in an external potential U follows the Langevin equation

$$\frac{dx_\alpha(t)}{dt} = -kx_\alpha(t) + \xi_\alpha(t), \quad (4)$$

driven by fractional Gaussian noise $\xi_\alpha(t)$ of zero mean $\langle \xi_\alpha(t) \rangle = 0$ and slowly decaying, power-law autocorrelation ($t \neq t'$) [23, 24]

$$\langle \xi_\alpha(t) \xi_\alpha(t') \rangle \simeq \alpha K_\alpha (\alpha - 1) |t - t'|^{\alpha-2}. \quad (5)$$

In free space, $\langle x_\alpha^2(t) \rangle = 2K_\alpha t^\alpha$ [14]. Note the change of sign in Eq. (5) between antipersistent subdiffusion $0 < \alpha < 1$ and persistent superdiffusion $1 < \alpha < 2$. Different to subdiffusive CTRW processes with diverging waiting time scale, FBM does not exhibit ageing effects. In fact, the free space propagator is the Gaussian [25]

$$P(x, t) = \sqrt{\frac{1}{4\pi K_\alpha t^\alpha}} \exp\left(-\frac{x^2}{4K_\alpha t^\alpha}\right), \quad (6)$$

whose smooth shape contrasts the pronounced cusps at the initial position in subdiffusive CTRW processes [13, 18]. Moreover, the propagator (6) obeys a time-local diffusion equation with time-dependent diffusivity [25].

The formal solution of the FBM-Langevin equation (4),

$$x_\alpha(t) = \int_0^t e^{-k(t-t')} \xi_\alpha(t') dt', \quad (7)$$

and Eq. (5) yield the position autocorrelation function

$$\begin{aligned} \langle x_\alpha(t_1) x_\alpha(t_2) \rangle &= K_\alpha \left\{ e^{-kt_2} t_2^\alpha + e^{-kt_1} t_1^\alpha - |t_2 - t_1|^\alpha \right\} \\ &+ \frac{K_\alpha}{2k^\alpha} \left\{ e^{-k|t_2-t_1|} \gamma(\alpha+1, kt_1) \right. \\ &\quad + e^{k|t_2-t_1|} \gamma(\alpha+1, kt_2) \\ &\quad \left. - e^{k|t_2-t_1|} \gamma(\alpha+1, k|t_2-t_1|) \right\} \\ &+ \frac{kK_\alpha}{2(\alpha+1)} |t_2 - t_1|^{\alpha+1} e^{-k|t_2-t_1|} \\ &\quad \times M(\alpha+1; \alpha+2; k|t_2-t_1|) \\ &- \frac{kK_\alpha}{2(\alpha+1)} t_1^{\alpha+1} e^{-k(t_1+t_2)} M(\alpha+1; \alpha+2; kt_1) \\ &- \frac{kK_\alpha}{2(\alpha+1)} t_2^{\alpha+1} e^{-k(t_1+t_2)} M(\alpha+1; \alpha+2; kt_2). \quad (8) \end{aligned}$$

For the EA MSD we then find

$$\begin{aligned} \langle x_\alpha^2(t) \rangle &= \frac{K_\alpha}{k^\alpha} \gamma(\alpha+1, kt) + 2K_\alpha t^\alpha e^{-kt} \\ &- \frac{kK_\alpha}{\alpha+1} t^{\alpha+1} e^{-2kt} M(\alpha+1; \alpha+2; kt), \quad (9) \end{aligned}$$

where $\gamma(z, x) = \int_0^x dt e^{-t} t^{z-1}$ is the incomplete γ function and

$$M(a; b; z) = \frac{\Gamma(b)}{\Gamma(b-a)\Gamma(a)} \int_0^1 e^{zt} t^{a-1} (1-t)^{b-a-1} dt \quad (10)$$

is the Kummer function [22]. Fig. 2 shows simulations of FBM in an harmonic potential for various α values, demonstrating excellent agreement with result (9). Asymptotic expansion of Eq. (9) at short times $t \ll k^{-1}$ yields free anomalous diffusion $\langle x_\alpha^2(t) \rangle \sim 2K_\alpha t^\alpha$. Close to stationarity, we find

$$\langle x_\alpha^2(t) \rangle \sim \langle x_\alpha^2 \rangle_{th} - \frac{2}{k^2} \alpha(\alpha-1) K_\alpha t^{\alpha-2} e^{-kt}, \quad (11)$$

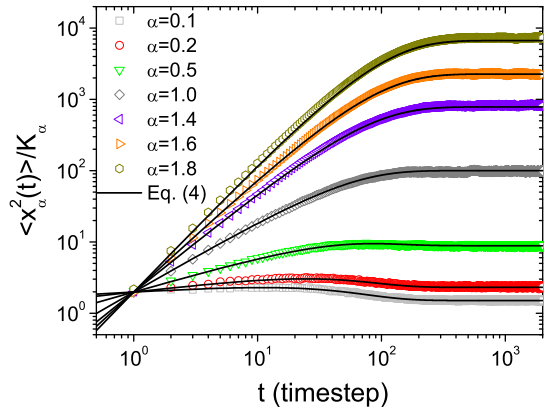


FIG. 2: EA MSD $\langle x_\alpha^2(t) \rangle$ for FBM in a harmonic potential. Solid lines: Eq. (9). Symbols: simulations with parameters $k = 0.01$, $T = 2048$, and $x_0 = 0$.

exponentially approaching the stationary value

$$\langle x_\alpha^2 \rangle_{\text{th}} = \frac{K_\alpha}{k^\alpha} \Gamma(\alpha + 1) \quad (12)$$

with the single characteristic time scale k^{-1} in the exponential function: as observed in Fig. 2, beyond $t > k^{-1}$ the stationary state is attained independent of α . This property enables one to study the confinement effect by analyzing the relaxation of $\langle x_\alpha^2(t) \rangle$. We also note an interesting feature of the relaxation dynamics in the intermediate timescale: somewhat counterintuitively the subdiffusive particle overshoots $\langle x_\alpha^2 \rangle_{\text{th}}$ before a depression back to this value, while for superdiffusion we observe a monotonic increase (the sign of the second term in Eq. (11) depends on α). Note that the α -dependence of the plateau value (12), a reminder of the fact that FBM is driven by an external noise and thus not subject to the fluctuation dissipation theorem, in contrast to FLE motion discussed below. Phenomenologically, both processes are very similar.

For the TA MSD in the limit $T \rightarrow \infty$ we obtain the expression

$$\begin{aligned} \overline{\delta^2(\Delta)} &= 2K_\alpha \Gamma(\alpha + 1) / k^\alpha + 2K_\alpha \Delta^\alpha \\ &- \frac{K_\alpha}{k^\alpha} \{ e^{k\Delta} \Gamma(\alpha + 1, k\Delta) + e^{-k\Delta} \Gamma(\alpha + 1) \} \\ &- \frac{kK_\alpha}{\alpha + 1} \Delta^{\alpha+1} e^{-k\Delta} M(\alpha + 1; \alpha + 2; k\Delta), \end{aligned} \quad (13)$$

where $\Gamma(z, x) = \int_x^\infty dt e^{-t} t^{z-1}$ is the complementary incomplete γ function. Comparison with the EA MSD, Eq. (9), demonstrates a completely different functional behavior *over all time scales*, except in the short-time limit for which confinement is negligible. In particular, at $\Delta \rightarrow \infty$, we find $\overline{\delta^2(\Delta)} = 2\langle x_\alpha^2 \rangle_{\text{th}}$ for all α .

The fundamental difference of the relaxation dynamics of $\overline{\delta^2(\Delta)}$ and $\langle x_\alpha^2(t) \rangle$ is evidenced in Fig. 3, in excellent

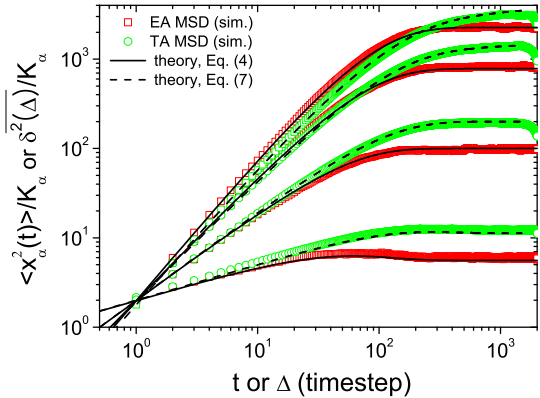


FIG. 3: EA and TA MSD, $\langle x_\alpha^2(t) \rangle / K_\alpha$ and $\overline{\delta^2(\Delta)} / K_\alpha$ for FBM in a harmonic potential ($\alpha = 0.40, 1.0, 1.4, 1.60$, bottom to top). Solid and dashed lines: analytical results (9) and (13). Symbols: simulations. Parameters as in Fig. 2.

agreement with Eqs. (9) and (13). In contrast to the exponential relaxation of Eq. (9), the TA MSD shows a power-law approach to the limiting value $2\langle x_\alpha^2 \rangle_{\text{th}}$, except for the Brownian limit $\alpha = 1$. This is manifested in the asymptotic form of $\overline{\delta^2(\Delta)}$ at $\Delta \rightarrow \infty$,

$$\begin{aligned} \overline{\delta^2(\Delta)} &\sim 2\langle x_\alpha^2 \rangle_{\text{th}} - \frac{K_\alpha \Gamma(\alpha + 1)}{k^2} e^{-k\Delta} \\ &- \frac{2\alpha(\alpha - 1)K_\alpha}{k^2 \Delta^{2-\alpha}}. \end{aligned} \quad (14)$$

The transient second term becomes the leading order at $\alpha = 1$. Surprisingly, in Eq. (14) the relaxation dynamics is determined by the power exponent $\alpha - 2$. Moreover, no characteristic time scale exists beyond which the MSD could be regarded saturated. For subdiffusion, as the algebraic decay is relatively fast ($\sim \Delta^{-\kappa}$ with $1 < \kappa < 2$), the MSD appears saturated at sufficiently long measurement time. However, the superdiffusive MSD relaxes very slowly as α is closer to 2 ($\sim \Delta^{-\kappa}$ with $0 < \kappa < 1$). Due to this the corresponding MSD does not show saturation even at long measurement time T . Only in the limit $\Delta \rightarrow T$ the TA dips back to the plateau value of the EA. In typical experiments, however, this feature is obscured by poor statistics, and thus the relaxation time would likely be overestimated from the TA MSD.

III. FRACTIONAL LANGEVIN EQUATION

The FLE describes ergodic anomalous diffusion and fulfills the fluctuation-dissipation theorem [14]. In the potential U , the FLE motion $y_\alpha(t)$ follows the dynamic

equation [14, 26, 28]

$$m \frac{d^2 y_\alpha(t)}{dt^2} = -\gamma \int_0^t dt' |t-t'|^{\alpha-2} \frac{dy_\alpha}{dt'} - k y_\alpha(t) + \sqrt{\gamma/[\alpha(\alpha-1)\beta K_\alpha]} \xi_\alpha(t), \quad (15)$$

where $\xi_\alpha(t)$ represents fractional Gaussian noise, m is the particle mass and γ the generalized friction coefficient. In the FLE, the dynamic exponent of the noise is restricted to $1 < \alpha < 2$. This persistent noise results in subdiffusive motion of the FLE in the overdamped limit. For unbiased motion ($k = 0$), $\langle y_\alpha^2(t) \rangle = \overline{\delta^2(t)}$ at $T \rightarrow \infty$ [14], and

$$\overline{\delta^2(\Delta)} = \frac{2\Delta^2}{\beta m} E_{\alpha,3} \left[-\Gamma(\alpha-1) \frac{\gamma}{m} \Delta^\alpha \right], \quad (16)$$

$E_{\alpha,3}(z)$ being a generalized Mittag-Leffler function. The latter is defined via its Laplace image

$$\int_0^\infty e^{-ut} E_{\rho,\delta}(-\eta^* t^\alpha) = \frac{1}{u^\delta + \eta^* u^{1-\alpha}}. \quad (17)$$

In terms of a series expansion around $z = 0$ and $z \rightarrow \infty$ this function reads [27]

$$E_{\rho,\delta}(z) = \sum_{n=0}^{\infty} \frac{z^n}{\Gamma(\delta + \rho n)} = -\sum_{n=1}^{\infty} \frac{z^{-n}}{\Gamma(\delta - \rho n)}. \quad (18)$$

The MSD (16) accordingly turns from ballistic motion $\sim \Delta^2$ at short Δ to subdiffusion $\sim \Delta^{2-\alpha}$ at long Δ [26, 28]. In the presence of the potential, the FLE (15) can be solved analytically in the overdamped limit, the stationary state yielding [28]

$$\langle y_\alpha(t_1) y_\alpha(t_2) \rangle_{\text{th}} = \frac{1}{\beta k} E_{2-\alpha} \left[-\frac{k}{\gamma \Gamma(\alpha-1)} |t_2 - t_1|^{2-\alpha} \right], \quad (19)$$

with $E_{2-\alpha}(z) = E_{2-\alpha,1}$. Thus, $\langle y_\alpha^2(t) \rangle$ has the stationary value $\langle y_\alpha^2 \rangle_{\text{th}} = 1/(\beta k)$ for any α , contrasting the α -dependent result (12) for FBM. Moreover for $T \rightarrow \infty$ we obtain the TA MSD

$$\overline{\delta^2(\Delta)} = 2 \langle y_\alpha^2 \rangle_{\text{th}} \left(1 - E_{2-\alpha} \left[-\frac{k}{\gamma \Gamma(\alpha-1)} \Delta^{2-\alpha} \right] \right) \quad (20)$$

for $\Delta \gtrsim \tau_c$, where the momentum relaxation time is [26]

$$\tau_c = \left(m \frac{\Gamma(\alpha+3)}{2\Gamma(\alpha-1)(2^{\alpha+1}-1)\gamma} \right)^{1/\alpha}. \quad (21)$$

The TA MSD (20) behaves distinctly different from its EA counterpart as well as the TA MSD (13) for FBM: the TA MSD (20) grows like $\sim \Delta^{2-\alpha}$ at intermediate lag time, and eventually converges to $2 \langle y_\alpha^2 \rangle_{\text{th}}$ for all α as $\Delta \rightarrow \infty$. Similar to our above observations, the long-time behavior of Eq. (20) exhibits a power-law relaxation, namely,

$$\overline{\delta^2(\Delta)} \approx 2 \langle y_\alpha^2 \rangle_{\text{th}} \left(1 - \frac{\gamma}{k \Delta^{2-\alpha}} \right). \quad (22)$$

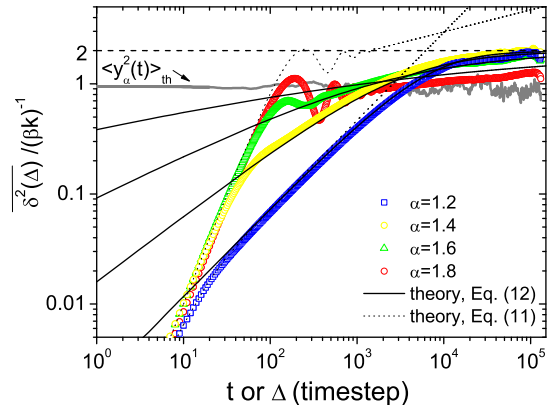


FIG. 4: TA MSD for FLE motion in an harmonic potential, for $\alpha = 1.2, 1.4, 1.6$, and 1.8 (bottom to top), and $T = 2^{17}$. A representative EA MSD is included for $\alpha = 1.2$. Symbols: Simulations with time step $\delta t = 0.001$, stiffness $k = 100$, mass $m = 1$, friction coefficient $\gamma = 100$, and $\beta = 1$, with equilibrium distribution of initial position $y_\alpha(0)$ and velocity $\dot{y}_\alpha(0)$. Full lines: theoretical result (20). Dotted lines: unbiased motion, Eq. (16), with momentum relaxation at $\alpha = 1.4$ and 1.8 , illustrating ballistic scaling $\sim \Delta^2$ at $\Delta < \tau_c$.

As for FBM, the dynamic exponent of the TA MSD is independent of the confinement (k). Intriguingly the speed of convergence is slower as the driving noise ξ_α is more persistent (i.e., when $\alpha \rightarrow 2$). Therefore, opposite to the tendency shown in Fig. 3 for FBM, in the FLE case the slow particle appears not to approach $2 \langle y_\alpha^2 \rangle_{\text{th}}$.

In Fig. 4, we further analyze FLE motion in an harmonic potential in terms of the TA MSD for various α . For times $\Delta \gtrsim \tau_c$ and in the overdamped limit, the analytical form (20) agrees well with the simulations results for all cases. While the TA MSD approaches the thermal value $2 \langle y_\alpha^2 \rangle_{\text{th}}$ algebraically, in our simulation the slowest subdiffusive case (corresponding to $\alpha = 1.8$) does not show saturation even for long measurement times. At times less than τ_c the TA MSD shows quadratic scaling $\overline{\delta^2} \simeq \Delta^2$. The dynamics within this time range is explained well by the full solution of the free space motion (16), shown for $\alpha = 1.2$ and 1.8 . An important feature resulting from this inertia effect are the oscillations of $\overline{\delta^2}$ that are particularly pronounced as α approaches 2. These oscillations are intrinsic in the sense that they occur regardless of the confinement, due to the strong persistence in ξ_α and inertia effects [29].

IV. DISTRIBUTION OF TIME AVERAGED MEAN SQUARED DISPLACEMENTS

At finite sampling time T the TA MSD $\overline{\delta^2(\Delta, T)}$ is a random variable, even for ergodic processes such as Brownian motion, FBM, and FLE motion. In practice, this means that $\overline{\delta^2(\Delta, T)}$ shows pronounced trajectory-

to-trajectory variations. This stochasticity of $\overline{\delta^2}$ is measured by the scatter probability density $\phi(\xi)$, in which the dimensionless variable ξ is defined through [11]

$$\xi = \overline{\delta^2} / \langle \overline{\delta^2} \rangle. \quad (23)$$

Such scatter distributions are of Lévy stable type for subdiffusive CTRW processes with diverging characteristic time scale [11, 15, 20, 30, 31]. In Figs. 5-7 we show ϕ for free and confined FBM and FLE motion, with fixed bin size 0.1. Each graph shows the distributions at three different lag times Δ and α for given measurement time T . In each graph two sets of curves were shifted upwards for comparison, the shift value is indicated in the graphs.

A. FBM in an harmonic potential

On the Left of Fig. 5 we present the distributions of $\overline{\delta^2}$ for the data shown in Fig. 3. As expected from our previous study [30], the distributions are centered around the ergodic value $\xi = 1$ and become wider as the lag time Δ increases. The wider distribution at longer lag time means that the single TA MSD trajectories tend to be more erratic as Δ approaches T . A new finding is that at a fixed lag time $\Delta > 1$ the scatter distribution becomes broader as the motion is faster (i.e., growing α). This behavior is mainly due to the inherent property of FBM itself, as the same tendency is also found without potential (see left panel in Fig. 7). This dependence on α is attributed to the fact that FBM is a Gaussian stationary process in which the spatial displacement x for time difference Δ is governed by the distribution $\sim \exp(-x^2/[4K_H\Delta^\alpha])$. On the Right we show the corresponding distributions when the measurement time is increased to $T = 2^{17}$. The distributions now appear insensitive to α and Δ . The fact that they are less sharp than the analytically predicted Gaussian is due to the finite size effect of the binning, see below.

B. FLE motion in an harmonic potential

The left and right panels of Fig. 6 depict the distributions corresponding to the parameters used in Fig. 4, with $T = 2^{11}$ and 2^{17} , respectively. Note that the variation of α was restricted to the range [1.0, 2.0], as FLE motion is only well defined for subdiffusion. The anomalous diffusion exponent in this case is given by $\kappa = 2 - \alpha$ in terms of the scaling exponent α of the fractional Gaussian noise. Generally the distributions are bell-shaped. Notably, at fixed lag time the distribution of FLE motion tends to be wider as the overdamped motion becomes slower (i.e., for increasing α), as opposed to the case of FBM. We also observe that the distributions of FLE motion appear generally wider than those of FBM (e.g., Fig. 5 Left), for the fact that the initial values of position and velocity for

FLE were chosen as the corresponding equilibrium distributions. For the case of long measurement time (Right), the distributions again appear insensitive to α and Δ for the given bin size.

C. FBM & FLE motion in free space

To appreciate the effect of confinement on the distribution, we simulated free FBM and FLE motion for the same parameters as in Figs. 3 and 4. As shown in Fig. 7 in both cases, the scatter distributions manifest features consistent with the confined cases. Only the width of the distribution becomes narrower by the presence of the confining potential, in particular, at longer lag times.

D. Influence of bin size

Typically experimental probing windows are limited, and meaningful quantitative analysis requires more or less coarse binning. In the context of the scatter plots shown here this practically means that for a bin size of 0.1 the peak cannot exceed the value 10, for reasons of normalization, $\int_0^\infty \phi(\xi) d\xi = 1$. For simulations data we can arbitrarily increase the accuracy and thus reduce bin sizes while still maintaining good statistics. Such a result is shown in Fig. 8 for bin size 0.01. For this resolution we may compare the shape of the distribution $\phi(\xi)$ determined from simulations with the theoretical approximation valid for short lag times Δ ,

$$\phi(\xi) \approx \sqrt{\frac{T - \Delta}{4\pi\tau^*}} \exp\left(-\frac{(\xi - 1)^2(T - \Delta)}{4\tau^*}\right), \quad (24)$$

as derived in Ref. [30]. Here, the scale τ^* is only introduced to account for correct dimensions and can be taken to one [time unit], compare Ref. [30]. The graph shows nice agreement with the measured data from the simulations. Interestingly the agreement is somewhat better in the confined case. At larger Δ the distribution becomes wider than predicted by Eq. (24), due to the strong correlation in successive square displacements, $[x(t + \Delta) - x(t)]^2$ (see Ref. [30]), and the curves split up for the different α .

V. DISCUSSION

Studying the representative example of ergodic FBM and FLE motion in an external harmonic potential we demonstrated that the TA MSD behaves significantly different from the EA MSD. Thus, naive interpretation of single trajectory time averages based on the knowledge of the ensemble behavior may lead to false conclusions on the physics underlying the observed motion. This so far overlooked discrepancy is particularly relevant for the relaxation behavior: while for the EA MSD the relaxation

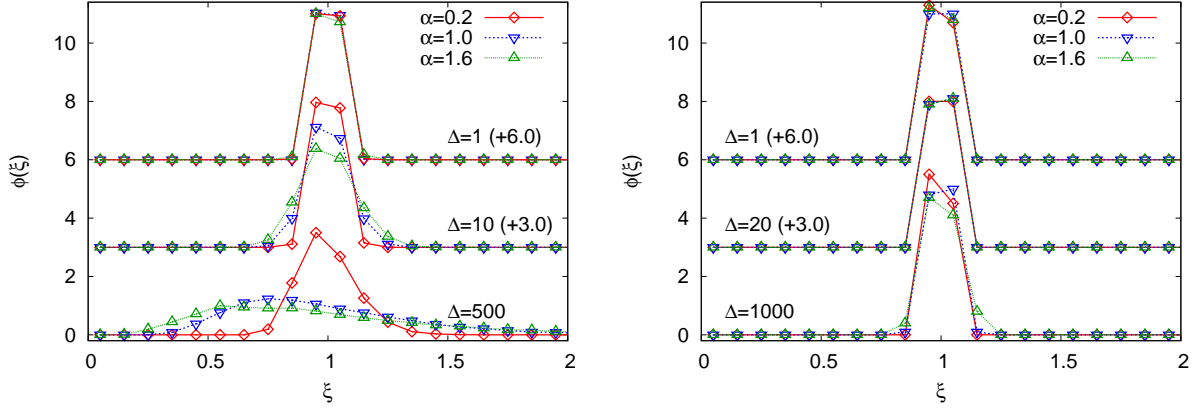


FIG. 5: Scatter distributions for fractional Brownian motion in an harmonic potential. Left: $T = 2^{11} = 2,048$. Right: $T = 2^{17} = 13,1072$. In each graph we compare the results for three different lag times. The two upper sets of curves were shifted by the indicated amount, for clarity.

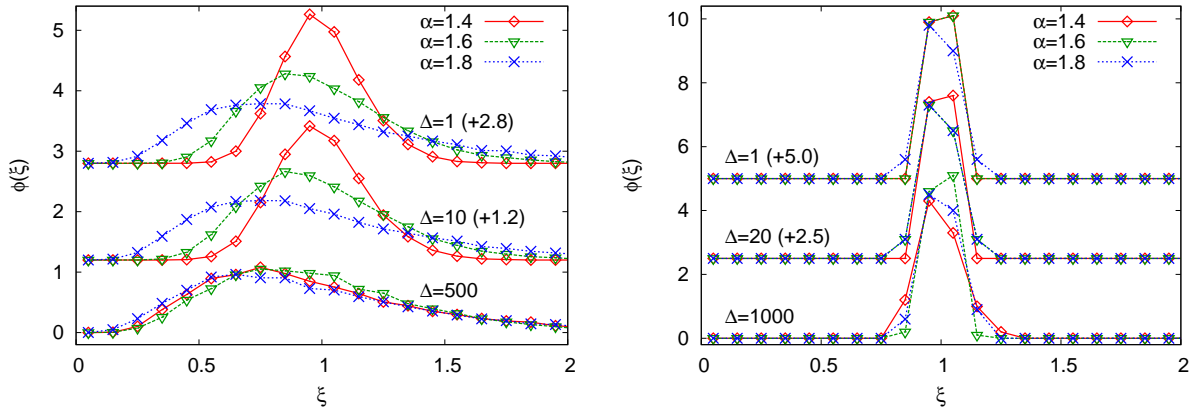


FIG. 6: Scatter distributions for fractional Langevin equation motion in an harmonic potential. Left: $T = 2^{11}$. Right: $T = 2^{17}$. In each graph we compare the results for three different lag times. The two upper sets of curves were shifted by the indicated amount, for clarity.

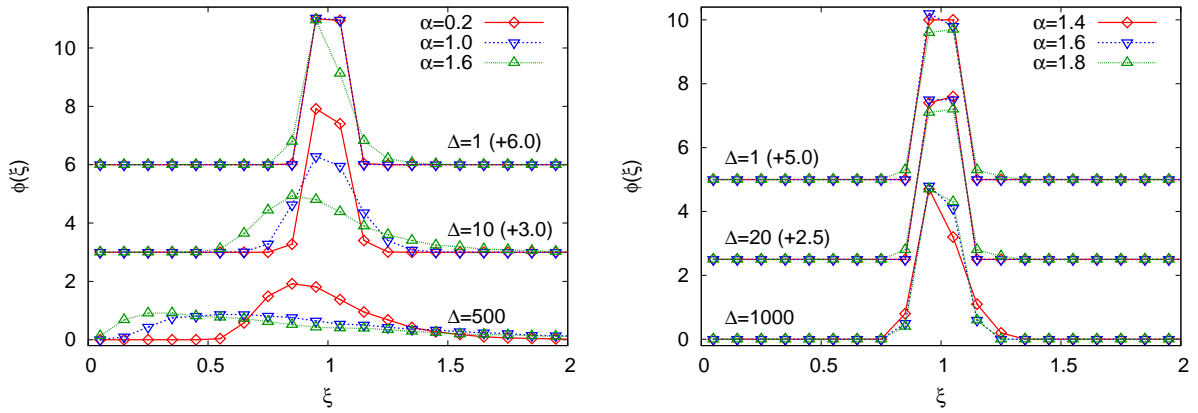


FIG. 7: Scatter distributions for free fractional Brownian and Langevin equation motion. Left: $T = 2^{11}$. Right: $T = 2^{17}$. In each graph we compare the results for three different lag times. The two upper sets of curves were shifted by the indicated amount, for clarity.

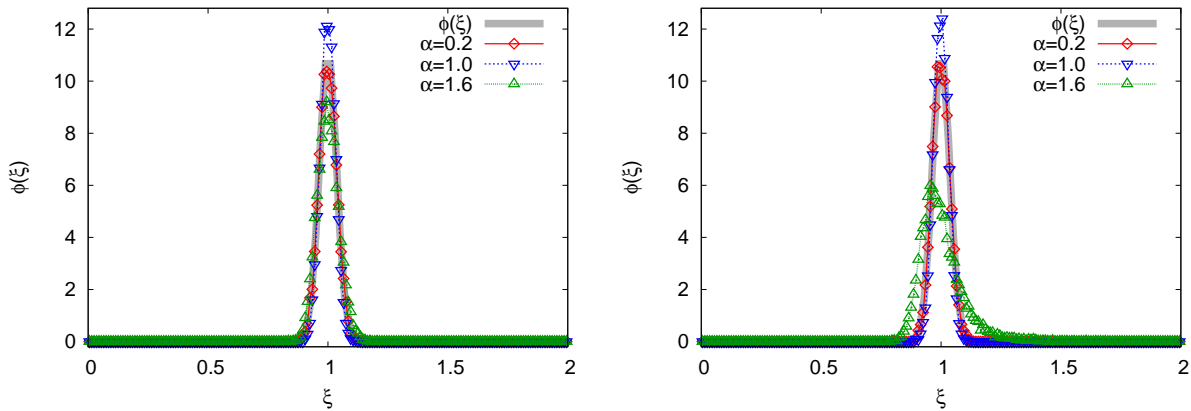


FIG. 8: Scatter distribution for confined (Left) and free (Right) FBM with $T = 2^{11}$, and $\Delta = 1$. Data are the same as shown in Figs. 5 and 7 to the Left, but analyzed with bin size 0.01. As shown by the grey line the measured scatter nicely agrees with the predicted Gaussian distribution (24).

time can be read off directly, the corresponding TA MSD appears to suggest a scale-free behavior. Hence it is imperative to compare to analytical or simulations results for the TA of the system. We note that while here we focused on an harmonic external potential, the findings reported here also pertain to other forms of confinement.

What is the reason for this disagreement between EA and TA? We find that for stochastic processes converging to a stationary state, as $\langle [x(t+\Delta) - x(t)]^2 \rangle_{\text{th}}$ only depends on Δ , the definition of the TA MSD (1) in the limit of long-time measurement leads to the general relation

$$\lim_{T \rightarrow \infty} \overline{\delta^2(\Delta, T)} = 2 \langle x^2 \rangle_{\text{th}} [1 - C_x(\Delta)], \quad (25)$$

which is independent of diffusion models and details of confinement. Here

$$C_x(\Delta) = \frac{\langle x(t)x(t+\Delta) \rangle_{\text{th}}}{\langle x^2 \rangle_{\text{th}}} \quad (26)$$

is the normalized position autocorrelation function. Therefore, the time-averaged variable $\overline{\delta^2(\Delta)}$ in fact is an indicator of the correlation of the spatial displacement, not the TA MSD of a trajectory. For ergodic systems satisfying the Khinchin theorem ($C_x(\Delta \rightarrow \infty) = 0$), the TA MSD always saturates to $\overline{\delta^2} \rightarrow 2 \langle x^2 \rangle_{\text{th}}$, where the relaxation dynamics reflecting the spatial correlation can be very slow although the system is already fully relaxed, as shown in this study. Accordingly, in performing single trajectory analysis, one should be aware of the potential pitfalls in using $\overline{\delta^2(\Delta)}$. In contrast to non-ergodic systems [11, 15, 20], the anomalous diffusion exponent α and the anomalous diffusion constant K_α can be estimated from the log-log plot of the TA MSD at short lag times. Meanwhile, physical quantities associated with confinement such as the effective confinement size and the relaxation time could be incorrectly deduced from the long- Δ behavior of $\overline{\delta^2(\Delta)}$.

What alternative definitions of the TA MSD could be used to mend this problem? Instead of Eq. (1) it would

be a straightforward idea to consider

$$\overline{x^2(t)} = \frac{1}{t} \int_0^t x^2(t') dt' \quad (27)$$

For ergodic processes with a stationary state, $\overline{x^2(t)}$ at $t \rightarrow \infty$ equals

$$\langle x^2 \rangle_{\text{th}} = \int x^2 e^{-\beta U(x)} dx / \int e^{-\beta U(x)} dx. \quad (28)$$

However, the time dependence of $\overline{x^2(t)}$ is different from that of $\langle x^2(t) \rangle$. Even for free diffusion exhibiting $\langle x^2(t) \rangle = 2K_\alpha t^\alpha$, the ensemble mean of $\overline{x^2(t)}$ is $\frac{2K_\alpha}{\alpha+1} t^\alpha$, and thus this definition does not even work for the Brownian case. If a dynamic variable like the MSD as function of time is concerned, it appears that no systematic way exists for defining a TA expectation compatible with the analogous EA.

For finite measurement time T the TA MSD $\overline{\delta^2}$ shows trajectory-to-trajectory variations, even for Brownian motion. Consistent with previous findings [30] for ergodic processes, the distributions are centered around the ergodic value $\xi = 1$. Importantly, in all cases the distribution is almost independent of confinement, except for some narrowing at long lag times. For both FBM and FLE at long T the distributions converge, while for shorter T a dependence on α prevails.

Concluding, the study of single trajectory averages is a non-trivial extension of the theory of stochastic processes knowledge of which is necessary to establish quantitative models for diffusion-limited processes in small complex systems. The current work contributes to the development of such a theory, and to a toolbox of diagnosis methods of the exact stochastic mechanism underlying experimental single particle trajectories [4, 7, 10, 32–34].

Acknowledgments

We thank E. Barkai and O. Pulkkinen for stimulating discussions. Financial support from the Academy of

Finland (FiDiPro scheme) is gratefully acknowledged.

-
- [1] C. Bräuchle, D. C. Lamb, and J. Michaelis, *Single particle tracking and single molecule energy transfer*, (Wiley-VCH, Weinheim, 2010); X. S. Xie *et al.*, *Annu. Rev. Biophys.* **37**, 417 (2008).
- [2] I. Golding and E. C. Cox, *Phys. Rev. Lett.* **96** 098102 (2006).
- [3] S. C. Weber, A. J. Spakowitz, and J. A. Theriot, *Phys. Rev. Lett.* **104**, 238102 (2010).
- [4] J.-H. Jeon, V. Tejedor, S. Burov, E. Barkai, C. Selhuber-Unkel, K. Berg-Sørensen, L. Oddershede, and R. Metzler, *Phys. Rev. Lett.* **106**, 048103 (2011).
- [5] G. Seisenberger, M. U. Ried, T. Endreß, H. Büning, M. Hallek, and C. Bräuchle, *Science* **294**, 1929 (2001).
- [6] I. Bronstein, Y. Israel, E. Kepten, Y. Shav-Tal, E. Barkai, and Y. Garini, *Phys. Rev. Lett.* **103**, 018102 (2009).
- [7] A. V. Weigel, B. Simon, M. M. Tamkun, and D. Krapf, *Proc. Nat. Acad. Sci. USA* **108**, 6438 (2011).
- [8] S. C. Kou and X. S. Xie, *Phys. Rev. Lett.* **93**, 180603 (2004); A. Taloni, A. V. Chechkin, and J. Klafter, *Phys. Rev. Lett.* **104**, 160602 (2010) and Refs. therein; L. Lizana, T. Ambjörnsson, A. Taloni, E. Barkai, and M. A. Lomholt, *Phys. Rev. Lett.* **81**, 051118 (2010).
- [9] J. Szymanski and M. Weiss, *Phys. Rev. Lett.* **103**, 038102 (2009).
- [10] M. Magdziarz, A. Weron, K. Burnecki, *Phys. Rev. Lett.* **103**, 180602 (2009).
- [11] Y. He, S. Burov, R. Metzler, and E. Barkai, *Phys. Rev. Lett.* **101**, 058101 (2008).
- [12] A. Lubelski, I. M. Sokolov, and J. Klafter, *Phys. Rev. Lett.* **100**, 250602 (2008).
- [13] R. Metzler and J. Klafter, *Phys. Rep.* **339**, 1 (2000); *J. Phys. A* **37**, R161 (2004).
- [14] W. Deng and E. Barkai, *Phys. Rev. E* **79**, 011112 (2009).
- [15] S. Burov, J.-H. Jeon, R. Metzler, and E. Barkai, *Phys. Chem. Chem. Phys.* **13**, 1800 (2011).
- [16] I. Goychuk, *Phys. Rev. E* **80**, 046125 (2009).
- [17] E. W. Montroll and G. H. Weiss, *J. Math. Phys.* **6**, 167 (1965).
- [18] H. Scher and E. W. Montroll, *Phys. Rev. B* **12**, 2455 (1975).
- [19] The related concept of weak ergodicity breaking was developed by Bouchaud and subsequently by Barkai and coworkers: J.-P. Bouchaud, *J. Phys. I* **2**, 1705 (1992); G. Bel and E. Barkai, *Phys. Rev. Lett.* **94**, 240602 (2005); A. Rebenshtok and E. Barkai, *ibid.* **99**, 210601 (2007). The consequences for the mixing behavior between boundaries and bulk diffusion were explored by M. A. Lomholt, I. M. Zaid, and R. Metzler, *Phys. Rev. Lett.* **98**, 200603 (2007).
- [20] S. Burov, R. Metzler, and E. Barkai, *Proc. Natl. Acad. Sci. USA* **107**, 13228 (2010).
- [21] T. Neusius, I. M. Sokolov, and J. C. Smith, *Phys. Rev. E* **80**, 011109 (2009).
- [22] M. Abramowitz and I. A. Stegun, *Handbook of Mathematical Functions* (Dover, New York, NY, 1972).
- [23] A. N. Kolmogorov, *Dokl. Acad. Sci. USSR* **26**, 115 (1940); B. B. Mandelbrot and J. W. van Ness, *SIAM Rev.* **1**, 422 (1968).
- [24] O. Yu. Sliusarenko, V. Yu. Gonchar, A. V. Chechkin, I. M. Sokolov, and R. Metzler, *Phys. Rev. E* **81**, 041119 (2010).
- [25] E. Lutz, *Phys. Rev. E* **64**, 051106 (2001).
- [26] J.-H. Jeon and R. Metzler, *Phys. Rev. E* **81**, 021103 (2010).
- [27] A. Erdélyi, Editor, *Higher Transcendental Functions*, Bateman Manuscript Project Vol. (McGraw Hill, New York, NY, 1954).
- [28] S. C. Kou, *Ann. Appl. Stat.* **2**, 501 (2008).
- [29] A variety of oscillatory behaviors occur in $\langle y_\alpha(0)y_\alpha(t) \rangle$ by combined effects of the memory of fractional noise and confinement [S. Burov and E. Barkai, *Phys. Rev. Lett.* **100**, 070601 (2008); *Phys. Rev. E* **78**, 031112 (2008)].
- [30] J.-H. Jeon and R. Metzler, *J. Phys. A* **43**, 252001 (2010).
- [31] I. M. Sokolov, E. Heinsalu, P. Hänggi, and I. Goychuk, *Europhys. Lett.* **86**, 30009 (2009).
- [32] V. Tejedor, O. Bénichou, R. Voituriez, R. Jungmann, F. Simmel, C. Selhuber-Unkel, L. Oddershede, and R. Metzler, *Biophys. J.* **98**, 1364 (2010).
- [33] T. Akimoto, E. Yamamoto, K. Yasuoka, Y. Hirano, and M. Yasui, *Phys. Rev. Lett.* **107**, 178103 (2011).
- [34] S. Condamin, V. Tejedor, R. Voituriez, O. Bénichou, and J. Klafter, *Proc. Natl. Acad. Sci. USA* **105**, 5675 (2008).